

Relationships between Moderate Resolution Imaging Spectroradiometer water indexes and tower flux data in an old-growth conifer forest

Yen-Ben Cheng,^{ab*} Sonia Wharton,^b Susan L. Ustin,^{ab} Pablo J. Zarco-Tejada,^a Matthias Falk,^b and Kyaw Tha Paw U^b

^aCenter for Spatial Technology and Remote Sensing, University of California, Davis, Davis, California 95616, USA

^bDepartment of Land, Air and Water Resources, University of California, Davis, Davis, California 95616, USA

*ybcheng@cstars.ucdavis.edu

Abstract. Methods to accurately estimate the biophysical and biochemical properties of vegetation are a major research objective of remote sensing. We assess the capability of the MODIS satellite sensor to measure canopy water content and evaluate its relationship to ecosystem exchange (NEE) for an evergreen forest canopy. A time-series of three vegetation indexes were derived from MODIS data, the Normalized Difference Vegetation Index (NDVI), the Normalized Difference Water Index (NDWI), and the Normalized Difference Infrared Index (NDII), which were compared to physically based estimates of equivalent water thickness (EWT) from the airborne AVIRIS hyperspectral instrument over a temperate conifer forest in southwestern Washington. After cross-calibration of the imagery, water indexes derived from MODIS showed good agreement with AVIRIS EWT, while the NDVI was insensitive to water content variation. Three years of NEE data from eddy covariance measurements at the Wind River AmeriFlux tower were compared with the time series of MODIS indexes, which show seasonal water content has similar trajectory with NEE. In contrast, the MODIS NDVI time series did not yield a good relationship with NEE. This study demonstrates the potential to use MODIS water indexes for spatial and temporal NEE estimation at regional and global scales in appropriate ecosystems.

Keywords: MODIS, AVIRIS, equivalent water thickness, vegetation index, water index AmeriFlux, eddy covariance, net ecosystem exchange (NEE).

1 INTRODUCTION

Accurate spatially resolved and temporal estimates of canopy biochemistry and biophysical properties has become an important contributor to knowledge of plant physiological status. At regional to global scales these data are critical for estimating terrestrial surface fluxes and understanding impacts and feedbacks to climate change [1-4].

1.1 Vegetation Indexes Used to Estimate Canopy Physiological Condition

The first index to become widely used to estimate leaf and canopy properties was the Normalized Difference Vegetation Index (NDVI) [5], which relates reflectance in the red region of the electromagnetic spectrum, around 660 nm, and the near-infrared around 860 nm to vegetation condition. NDVI has been extensively used for two decades (>1600 published papers) to correlate to and/or estimate a wide range of plant properties including leaf area index [1, 6-8] and leaf mass [7, 9-13], chlorophyll (or pigment) concentration [11, 13-15], absorbed (or fraction) photosynthetic radiation [6, 8, 11, 16], % cover [17-19], among others.

An early theoretical study by Sellers [1, 16] showed the potential for NDVI to respond to canopy resistance and photosynthetic capacity over a realistic range of environmental conditions. This study was followed by incorporation of NDVI into a process model, the Simple Biosphere Model (SiB) [20] and later an improved SiB2 model [6, 21]. In particular, for sites with a strong seasonal phenology in leaf development, e.g. grasslands, NDVI has been demonstrated to be a good surrogate for LAI and FPAR in land surface models. Furthermore, because NDVI is correlated to canopy density or abundance, it can be used with land surface net radiation for modeling diurnal transpiration and photosynthesis, and produce estimates of regional scale CO₂ fluxes [22-24]. In a recent experimental climate change study, Filella *et al.* [25] followed seasonal and annual changes in CO₂ uptake in a mixed deciduous and evergreen Mediterranean shrubland for four years and demonstrated that NDVI could indirectly track temporal changes in CO₂ flux.

However, some studies show that NDVI is not always a good indicator of leaf area index or biomass and is not correlated with CO₂ uptake. There is little correlation between assimilation and NDVI in evergreen vegetation during climate periods that are adverse for growth. For example, Gamon *et al.* [11, 13] found that photosynthetic rates in evergreen forest and shrub communities have little correlation to NDVI during the summer drought in California when stomata are closed. Others have shown similar results under low winter temperatures [26, 27]. Conversely, under conditions of high productivity NDVI becomes saturated at high pigment concentrations and high leaf area, with saturation occurring at LAI of 3-4 in most ecosystems [1, 28, 29]. This saturation occurs substantially below the LAI typical of high productivity sites (where LAI is often >6), which are important sinks of carbon dioxide. Reliance on NDVI alone may under-estimate fluxes of CO₂ and water, which feedback into other physiological processes. NDVI is adversely affected by dense and multi-layered canopies, causing a strong non-linear relationship to green LAI [30, 31]. Moreover, NDVI is also affected by other factors such as variable soil background, canopy shadows, illumination, and atmospheric conditions [28, 32-36] that are common conditions in mature forests. A recent evaluation found that the MODIS Enhanced Vegetation Index (EVI) is more sensitive to canopy structure while NDVI is more sensitive to chlorophyll [33]. Although EVI and NDVI can both follow seasonal phenological timing, additional or revised remotely sensed measures of canopy properties are needed to (1) identify when NDVI may be wrong, (2) evaluate the temporal trajectory of canopy water indexes as an alternate physiological indicator in summer drought ecosystems, (3) provide constraints to modify vegetation indexes, and (4) more precisely estimate canopy physiological processes in evergreen ecosystems.

1.2 Water Content Indexes and Physiological Status

Canopy water content is of interest because of implications for drought stress monitoring in agriculture and forestry [12, 37-42]. In recent years, land surface parameterization has used modern theories that relate photosynthesis and evapotranspiration to provide consistent descriptions of water, energy, and carbon exchange between the vegetated land surface and the atmosphere in [43, 44]. Plant metabolism, based on the photosynthetic activities, requires an open pathway, stomata, for the transfer of CO₂ which leads to an inevitable water vapor loss from the canopy. Therefore, the linkage between water and carbon is based on the biophysical regulation of stomata, which involves optimization to maximize carbon fixed by photosynthesis, yet reduce water loss [6, 21, 44]. Turgor pressure governed by leaf hydration regulates stomatal opening.

Reflectance in the near-infrared and shortwave-infrared (1500-2500 nm) regions are largely influenced by water absorption [12, 38, 45, 46] therefore potentially providing a quantitative estimate of plant water content. Gao [12] proposed the Normalized Difference Water Index (NDWI) using the water absorption features at 860 nm and 1240 nm to retrieve

vegetation liquid water, and indicated potential usage of the Moderate Resolution Imaging Spectrometer (MODIS) band 2 (858.5nm) and band 5 (1240nm) for deriving NDWI and canopy water content. Subsequent studies support the estimation of canopy water content and possibly water stress monitoring using MODIS [39, 47, 48].

The MODIS product MOD09A1 (<http://modis-land.gsfc.nasa.gov/surfrad.htm>) provides calibrated reflectance for the seven 250m and 500m spectral bands in the 400 nm to 2500 nm spectral region at an eight-day composited temporal resolution. This coarse scale global reflectance product was built to provide continuous land cover characteristics at the regional scale and to explore its connection to global ecosystem processes, including the exchange of carbon, water, and energy between land surface and the atmosphere [2, 33, 42]. In this product, band 2, centered at 858.5 nm, band 5 at 1240 nm, and band 6 at 1640 nm have been used for retrieving water content information [12, 19, 39, 47-49]. Radiative transfer models such as PROSPECT [50] linked to canopy models show that other biochemical constituents such as dry matter content (cellulose, lignin, nitrogen, etc.) along with canopy structure and leaf area in addition to canopy water cause large effects on MODIS reflectance [39, 47], thus, the utility of a water index remains uncertain.

Although structure affects the quantitative retrieval of water content, other studies have demonstrated that NIR and SWIR band reflectances can produce good correlations between image based canopy water content and field measured water content for vegetation types ranging from wetlands to semiarid shrublands [38, 40, 51-53]. In the semiarid Sahelian zone of West Africa, Fensholt and Sanholt used the Shortwave Infrared Water Stress Index (SIWSI) from MODIS bands 2, 5, and 6 and showed a strong correlation to *in situ* surface soil moisture measurements [48]. The concept of this band combination was developed earlier by Hardisky *et al.* [54] for Landsat Thematic Mapper using the term Normalized Difference Infrared Index (NDII). A similar combination of NIR and SWIR bands was used by Xiao *et al.* [55] from SPOT-VGT, band 3 (780-890 nm) and the SWIR band (1580-1750 nm), as an indicator of vegetation and soil moisture, which was shown to identify distinct temporal growth patterns in temperate and boreal forests. This study showed NDWI had a larger dynamic range between vegetation types than NDVI and that NDWI was high in spring months (March to May) when NDVI was low, which was attributed to snow melt and cover differences. This water index was later derived from MODIS reflectance product band 2 and 6 under the name Land Surface Water Index (LSWI) [19, 49, 56] and used in a satellite-based Vegetation Photosynthesis Model to estimate the impact of seasonal dynamics of soil moisture on plant photosynthesis and along with the EVI, to estimate gross primary production (GPP) in a temperate deciduous forest [49] and in a tropical evergreen forest [56].

This manuscript extends progress on retrieval of MODIS canopy water content to a high LAI evergreen forest that experiences seasonal soil moisture restrictions that limit photosynthesis and transpiration. The MODIS water content index is compared to a theoretically derived water content estimate from the Airborne Visible/Infrared Imaging Spectrometer (AVIRIS) for validation. Then a three-year time series between the MODIS water indexes and eddy covariance data at the Wind River Canopy Crane Research Facility, Washington, USA is used to test the relationships between MODIS indexes and carbon dioxide, latent heat, and sensible heat fluxes. Lastly, the potential to use indexes to develop spatially and temporally resolved regional estimates of carbon sequestration is demonstrated.

2 METHODS AND DATA USED

2.1 Wind River Site Characteristics

The Wind River Canopy Crane Research Facility (WRCCRF) is located in the T.T. Munger Research Natural Area of the Gifford National Forest in southwestern Washington. The ancient Douglas-fir (*Pseudotsuga menziesii*) and western hemlock (*Tsuga heterophylla*)

dominated forest (1,740 trees ha⁻¹ with heights up to 65m) [57], and mean LAI of ~9.4 [58] is composed of eight conifer species of different ages (up to ~500 years old) and represents a high live biomass (39,800 gC m⁻²) [59] and structurally dense and complex mature conifer forest [60]. This is the oldest forest in the international FLUXNET measurement network and the ecosystem type is highly under-represented in terms of its environmental complexity within the AmeriFlux network [61].

The region is at a transition between a temperate marine climate to the west and a drier continental climate to the east and is within the transient snow zone of the Cascade Mountains, where winter rain-on-snow and freezing-rain events are common. Mean annual air temperature is 8.7°C and mean precipitation is 2223 mm yr⁻¹, based on 1978-1998 data from the Carson National Fish Hatchery, 5 km north of the canopy crane (National Oceanographic and Atmospheric Administration National Climate Data Center). Only 5% of annual precipitation falls during the summer and drought typically lasts 60-80 days between June, July and August [57]. The distinct wet and dry seasons are offset in time from seasonal phenological events that are in this regard, unique among the climate systems of other mature forests studied in the AmeriFlux network.

The WRCCRF maintains an 85-m tall construction crane within the old-growth forest (45°49'13.76"N and 121°57'06.88"W) that provides within canopy access for biometeorological, microclimatic, and ecological measurements over 2.3-ha area [62]. It is located approximately 1 km from the eastern edge of the old-growth forest and about 0.5 km from both the north and south edges of the forest.

2.2 Biometeorological Flux Measurements

Eddy-covariance instruments (Solent Gill HS 3-D sonic anemometer and fast-response Li-Cor 6262 infrared gas analyzer) were mounted on the crane at a height of 70m. Details about instrument methodology are described in Paw U *et al.* [63] and Falk [64]. Turbulent fluxes of carbon dioxide, latent heat, and sensible heat have been measured continuously since March 1998 although this study only includes flux data from 1 January 2001 to 31 December 2003 to correspond with the MODIS data. Flux data were processed to remove half-hourly measurements outside their expected ranges, to correct for low turbulent conditions and to gap-fill any missing data.

The widely reported u* correction method [65, 66] was used to correct nighttime CO₂ fluxes when turbulent friction velocity (u*) was less than 0.3 m s⁻¹ (the u*critical value). Nocturnal fluxes measured under low turbulent conditions must be corrected due to the possibility that weak turbulence signals are missed by the eddy-covariance sensors and the occurrence of mean vertical and horizontal advection, all of which can lead to an underestimation of nighttime CO₂ flux by the instrumentation.

Nighttime CO₂ fluxes under low turbulence conditions were replaced using an empirically derived respiration model, $F_{RE} = a \exp(b \cdot Ta_{02})$, where F_{RE} is the half-hourly CO₂ (respiration) flux, Ta_{02} is the air temperature at 2m, and a and b are coefficients specific to the data period. The respiration model is based on measured, high turbulent nocturnal CO₂ fluxes and is used to predict the respiratory flux based on air temperature for all nighttime half-hours when $u^* < u^*_{critical}$. This exponential relationship was found to overestimate ecosystem respiration fluxes under high temperatures and during times of soil moisture stress. To correct for this, a respiration-attenuation function was empirically derived and triggered for use in the nighttime respiration model when soil moisture measurements fell below ~ 0.23 m³ m⁻³ [64]. This was typically important during the summer months when high temperatures coincided with seasonal drought. Any missing nighttime CO₂ flux measurements were also gap-filled using the nighttime respiration model.

Missing daytime CO₂ fluxes were replaced using gap-filling algorithms developed by Reichstein *et al.* [67]. The gap-filling strategy considers both the relationship between fluxes

with meteorological data and their temporal autocorrelation and is an advanced implementation of the widely used Falge *et al.* [65] methodology. Half-hourly CO₂ flux measurements were also replaced if values were outside the expected range ($-35 \mu\text{mol} < \text{CO}_2 \text{ flux} < 25 \mu\text{mol}$), if the CO₂ flux variance was greater than the highest 95th percentile, during high precipitation events, and during times of general instrument failure.

Gross Primary Production (GPP) is estimated on a half-hourly basis as the residual between net ecosystem exchange (NEE) and total ecosystem respiration (TER), where $\text{GPP} = \text{NEE} - \text{TER}$. To estimate GPP, daytime respiration fluxes are first modeled. This is done using the temperature-based respiration model, including the water stress attenuation function, as used to correct the nighttime CO₂ fluxes (i.e., respiration fluxes) under low turbulent conditions. GPP is calculated as the difference between NEE, which is measured with eddy covariance instrumentation and TER and is integrated over 8 days.

2.3 Remote Sensing Data

2.3.1 AVIRIS Data

Airborne hyperspectral AVIRIS (Advanced Visible Infrared Imaging Spectrometer, <http://aviris.jpl.nasa.gov>) data flown at high spatial resolution were used to validate the water content measured by MODIS. AVIRIS measured 224 contiguous spectral bands in the 400 to 2500 nm spectral range with a spatial resolution of 4 m over the Wind River study site on 01 August 2002 and on 19 July 2003. Ground control points and spectral data collection were measured in the field at the time of the overflights using an ASD FieldSpec (Analytical Spectral Devices, Boulder, CO) spectrometer and ProXRS GPS (Trimble Navigation, Inc., Sunnyvale, CA) for georegistration. An atmospheric correction to convert the data from radiance to apparent surface reflectance was performed using ACORN (ImSpec LLC, Analytical Imaging and Geophysics LLC, Boulder, CO), a MODTRAN-4 (Spectral Sciences, Inc., Burlington, MA) based radiative transfer model, which was followed by application of an empirical line enhancement using ASD field spectra to remove additional artifacts in the AVIRIS data. To test the reflectance retrieval, the difference between atmospherically corrected AVIRIS spectra and ASD field measurements (not used in calibration) were found to be within 2.24% (SD=1.74%, RMSE=3.33%). Empirical evaluation of the AVIRIS data after atmospheric correction supports the quality and spectral integrity in the 400-2500 spectral data over the flightline region.

Retrievals of equivalent water thickness (EWT) from AVIRIS were made following the method of Green *et al.* [68, 69] and Roberts *et al.* [70], using the ACORN radiative transfer model. Because of a 40 nm spectral shift between the maximum wavelength for absorption by liquid water and water vapor, these phases of water can be simultaneously retrieved by fitting the measured pixel reflectance to the equivalent transmittance spectrum for a slab of water based on Beer-Lambert law [68-71].

Cross-calibration to MODIS data was performed on spatially and spectrally degraded AVIRIS images (to match MODIS resolutions), by selecting pixels from both AVIRIS and MODIS data that represented a wide range of reflectance values (e.g. a young forest pixel and a meadow pixel) which were used to develop an empirical regression for each spectral band. The mean reflectance of the 15625 AVIRIS pixels that corresponded to each MODIS pixel were calculated over the full extent of the AVIRIS flightline and extracted as simulated MODIS bands (band 1, band 2, band 5 and band 6).

2.3.2 MODIS Data

Eight-day MOD09A1 MODIS composite data was obtained from NASA Goddard Space Flight Center for the period 2001 through 2003. The data included the seven bands in the 400

nm to 2500 nm region measured at 500m pixel resolution, one data quality flag band that indicates cloud, snow, and aerosol conditions, and five other bands containing viewing geometry and state information. Band 2 (858.5 nm), band 5 (1240 nm), and band 6 (1640 nm) were used for retrieving water content information, and band 1 (645 nm) and band 2 (858.5 nm) were used for calculating NDVI. The data were filtered by the flagged data to remove cloud and snow covered pixels. For each of the major vegetation types at Wind River, an average value of NDVI, NDWI, and NDII was calculated for each eight-day period. Because of extensive cloud and snow cover, indexes could not be calculated in December and January so these data were removed from the analysis. NDWI is calculated following Equation 1 [12, 39] and NDII following Equation 2 [48, 54].

$$NDVI = \frac{Band2 - Band1}{Band2 + Band1} = \frac{R_{858.5} - R_{645}}{R_{858.5} + R_{645}} \quad (1)$$

$$NDWI = \frac{Band2 - Band5}{Band2 + Band5} = \frac{R_{858.5} - R_{1240}}{R_{858.5} + R_{1240}} \quad (2)$$

$$NDII = \frac{Band2 - Band6}{Band2 + Band6} = \frac{R_{858.5} - R_{1640}}{R_{858.5} + R_{1640}} \quad (3)$$

Cumulative index values were calculated from the difference in each value between two adjacent time dates, which represented changes of plant physiological properties (e.g. water content). Then the change in the index was accumulated through the year. These cumulative difference indexes were then compared with cumulative fluxes to develop empirical relationships between MODIS indexes and fluxes.

3 RESULTS

3.1 Eddy Covariance

The eight-daily fluxes for NEE (net ecosystem exchange of CO₂), GPP (Gross Primary Production), LE (latent heat) and H (sensible heat) and the cumulative fluxes for these properties calculated over the three years are shown in Fig. 1. The old-growth forest was a weak-to-moderate net sink for carbon during two (2001, 2002) of the three years (2001-2003) shown. Carbon flux measurements of this ancient forest show remarkably high interannual variability. The forest switched from being a moderate sink for carbon in 2002 (-98 gC m⁻² yr⁻¹) to a moderate source in 2003 (+100 gC m⁻² yr⁻¹) with no apparent change in leaf mass. This paper follows the biometeorological notation where a negative flux indicates that the ecosystem was a net sink for carbon, while a positive flux shows a net loss of carbon from the ecosystem to the atmosphere (i.e., the forest lost more carbon through respiration than it assimilated). The remaining components of NEE including canopy carbon storage, horizontal and vertical advection, and the undetectable vertical eddy flux of CO₂ are considered negligible based on the analysis by Paw U *et al.* [63] which is supported by modeling [72] and inventory methods [59]. Storage of carbon dioxide within the canopy is ignored because it is approximately zero after integrating over daily and annual time scales. While vertical and horizontal advection can dominant under low turbulence conditions at night, the u* correction methodology replaced questionable flux measurements for the analysis period. We identified the time frame during which the ecosystem functions as a carbon sink each year, which was Julian Day (JD) 45 to JD 195 in 2001, JD 30 to JD 180 in 2002, and JD 60 to JD 165 in 2003 (Fig. 1). This is the period when the ratio of gross primary productivity to total ecosystem respiration is greater than 1 (GPP/TER >1).

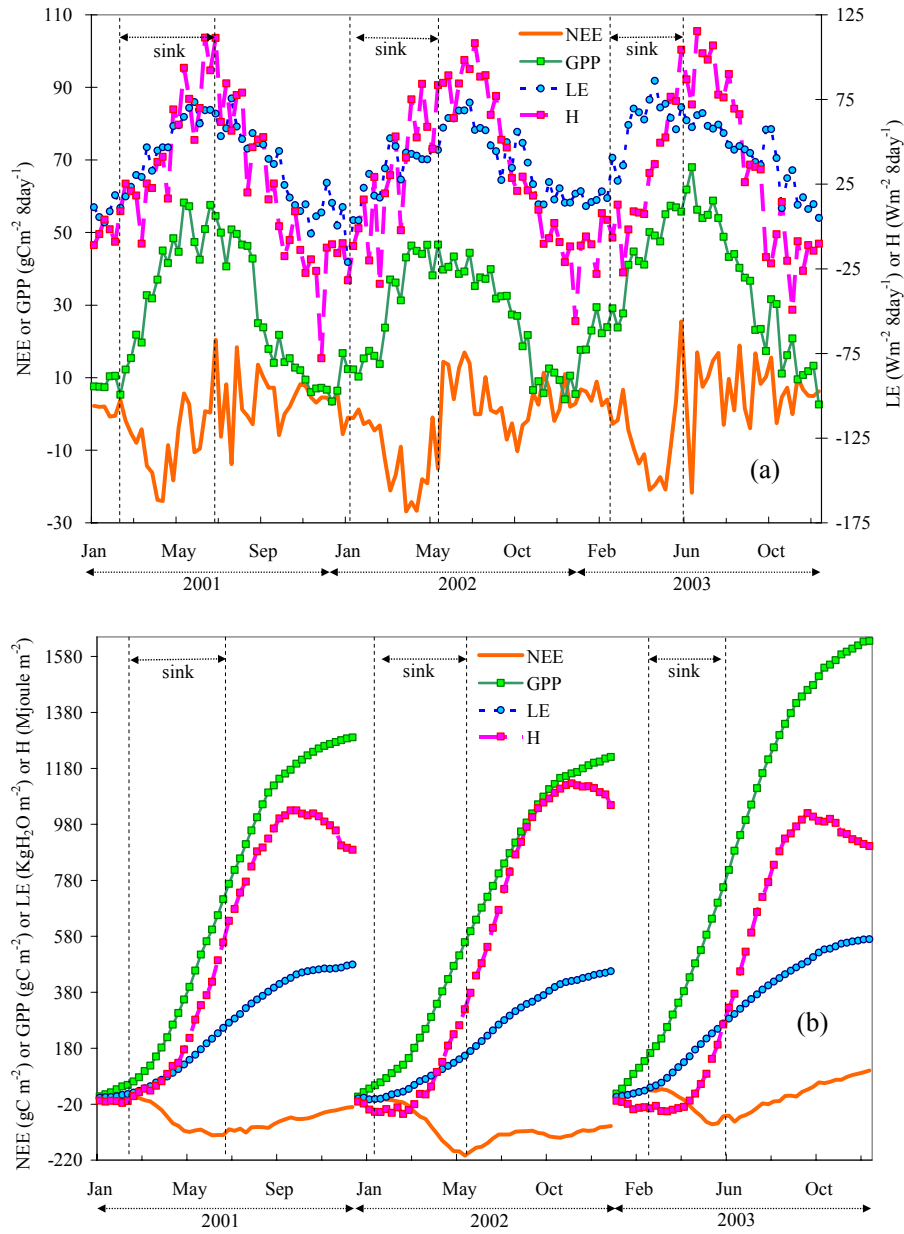


Fig. 1. (a) NEE, GPP, LE and H fluxes for three years (2001 through 2003) measured at the Wind River Canopy Crane AmeriFlux site. Dashed vertical lines indicate the length of the period each year that the forest was a sink for carbon. (b) Annual cumulative fluxes for NEE, GPP, LE, and H for three years (2001 through 2003) at the Wind River Canopy Crane AmeriFlux site.

Further analysis has shown that the sink strength in the old-growth forest ecosystem is very sensitive to perturbations in precipitation and temperature during the late spring and early summer months [64], which explains the high levels of interannual variability. In contrast to most mid-latitude deciduous forests (e.g. Harvard Forest; see Ref [73]) the Wind

River forest, like other conifer forests of the Pacific Northwest (e.g. British Columbia, Canada; see Ref [74]), experience maximum net carbon sink activity (greatest negative NEE values) during April and May rather than summer. Pacific Northwest conifers are adapted to low light and cool winter temperatures and tolerate the summer drought by partial dormancy, which allows high annual productivity in favorable climate years. Annual NEE at Wind River is closely correlated with the water-year (July to June) precipitation. Winter precipitation and melting of the snow pack provide maximum soil moisture in early spring when light and temperature conditions are most favorable for photosynthesis. Any shift in the end of the rainy season can either extend the maximum sink activity period into the summer (if winter precipitation is above normal) or limit and shorten the period of net carbon uptake (if winter precipitation is below normal). The impact of high precipitation was particularly evident in 1999 [63] when the net sink period extended late into August. Differences in annual NEE for 2001, 2002, and 2003 are probably related to summer and fall respiration rates which are driven by a combination of temperature and soil moisture, producing nonlinear ecosystem responses [75].

3.2 Precipitation and Temperature Data

Climate data collected at the NOAA Carson Fish Hatchery Station are shown in Fig. 2 for years 2001 through 2003. The annual average temperatures for the calendar years 2001 to 2003 were 8.72, 8.68, and 9.74°C, respectively, with annual precipitation of 1908 mm, 1970 mm, and 2230 mm. These data confirm that years 2001 and 2002 were at the long-term temperature average for the site although 2003 was on average 1°C higher. Precipitation totals are defined for water-years. To include the entire rainy season for these three calendar years, precipitation is 1247, 2446, 2130, and 1857 mm, for July 2000 to July 2004, respectively. The water year 2001 (for which January to July 2001 is within the MODIS measurement period) was a period of extreme drought (56% of normal precipitation) and was the lowest recorded precipitation since 1919. This was followed by two years of near normal precipitation, which in 2002 was 23mm (1%) above and 2003 was 92 mm (4%) below normal. The last six months of our measurement period, from July 2003 to January 2004 was the beginning period of another severe drought year which ultimately received only 83% of normal rainfall.

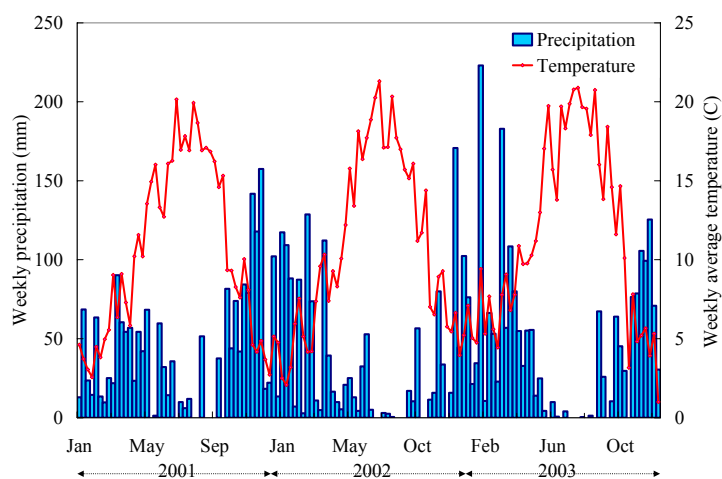


Fig. 2. Weekly average temperature and cumulative precipitation at Carson Fish Hatchery Station for three calendar years (2001 through 2003).

3.3 AVIRIS and MODIS Data Comparison

A comparison between canopy water content derived from the airborne high spatial resolution hyperspectral AVIRIS data was done to verify the MODIS index retrieval of canopy water content. Retrievals of EWT from AVIRIS were compared to MODIS water indexes on 01 August 2002 and 19 July 2003 to assess the effects of spatial and spectral resolution. The 937500 pixels in the 19 July 2003 AVIRIS image shown in Fig. 3a are equivalent to 60 MODIS pixels or 1500 ha. The color infrared image (Fig. 3a) shows that most of the area is vegetated although the patchiness illustrates the significant extent of logging and land use change in the area. The actual extent of the T.T. Munger Research Natural Area is the darker L-shaped zone, including the adjacent section of Trout Creek, in the lower right quadrant of the panel.

Visual assessment of AVIRIS reflectance spectra extracted from the imagery on 19 July 2003 after atmospheric correction (Fig. 3b) demonstrates the quality and spectral integrity of the data in the 400-2500 spectral range. Representative spectra of three forest types are shown for the mature old-growth forest, new growth i.e., regenerating conifer forest, and riparian forest (deciduous broadleaf forest species, e.g. red alder).

Because different vegetation types have structural and physiological characteristics that affect their optical properties, the study site was classified into five general land cover types (Fig. 3c), including the three major vegetation types of the area: mature old-growth conifer forest, regenerating conifer forests (young stands at the biomass accumulation/competitive exclusion stage; see Ref [60], and riparian forest (e.g. red alder). For each vegetation type, comparisons were made between MODIS water indexes and AVIRIS EWT measured over the site at the coincident time.

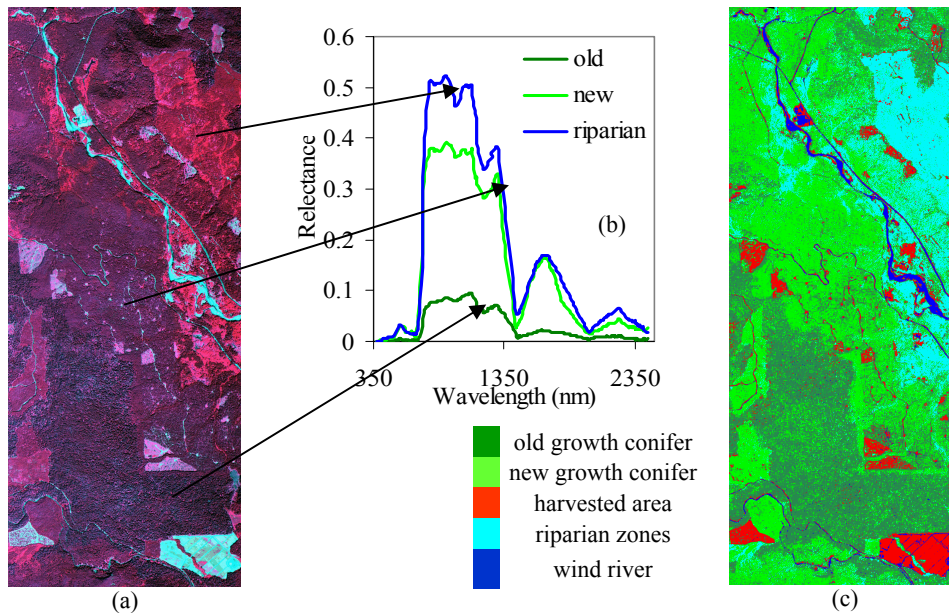


Fig. 3. (a) False color infrared image developed by AVIRIS imagery on 19 July 2003 at Wind River, (b) Reflectance features of the three major vegetation types, old growth conifer, new (regenerating) growth conifer, and riparian zones. Arrows point from the pixels where the spectra were obtained, (c) Vegetation map at Wind River developed with AVIRIS imagery (3a) using the vegetation GIS data base developed by Gifford Pinchot National Forest.

Equivalent water thickness (EWT) for nearly one-million pixels derived from AVIRIS data on 19 July 2003 is shown in Fig. 4a. This physically based measurement has been demonstrated to monitor spatial and temporal variation in water content in crops [76], woodland savanna [70], semi-arid shrublands [40, 53, 77] and conifer forests [29].

EWT was calculated in AVIRIS pixels coincident with the MOD09A1 image in 2002 and 2003. For each MODIS pixel the mean value of AVIRIS EWT ($n=15625$) was calculated. Fig. 4a shows the ACORN-derived EWT AVIRIS image on 19 July 2003 and Fig. 4b shows the 500 m averaged AVIRIS EWT (equivalent to MODIS pixels) with the corresponding NDWI and NDII images calculated from MODIS MOD09A1 reflectance, in Fig. 4c and 4d, respectively. The ACORN-derived AVIRIS EWT image on 1 August 2002 is shown in 3e and averaged at 500 m pixels in Fig. 4f, and corresponding MODIS NDWI and NDII images in Fig. 4g to Fig. 4h. In general it is possible to observe the same spatial patterns in AVIRIS

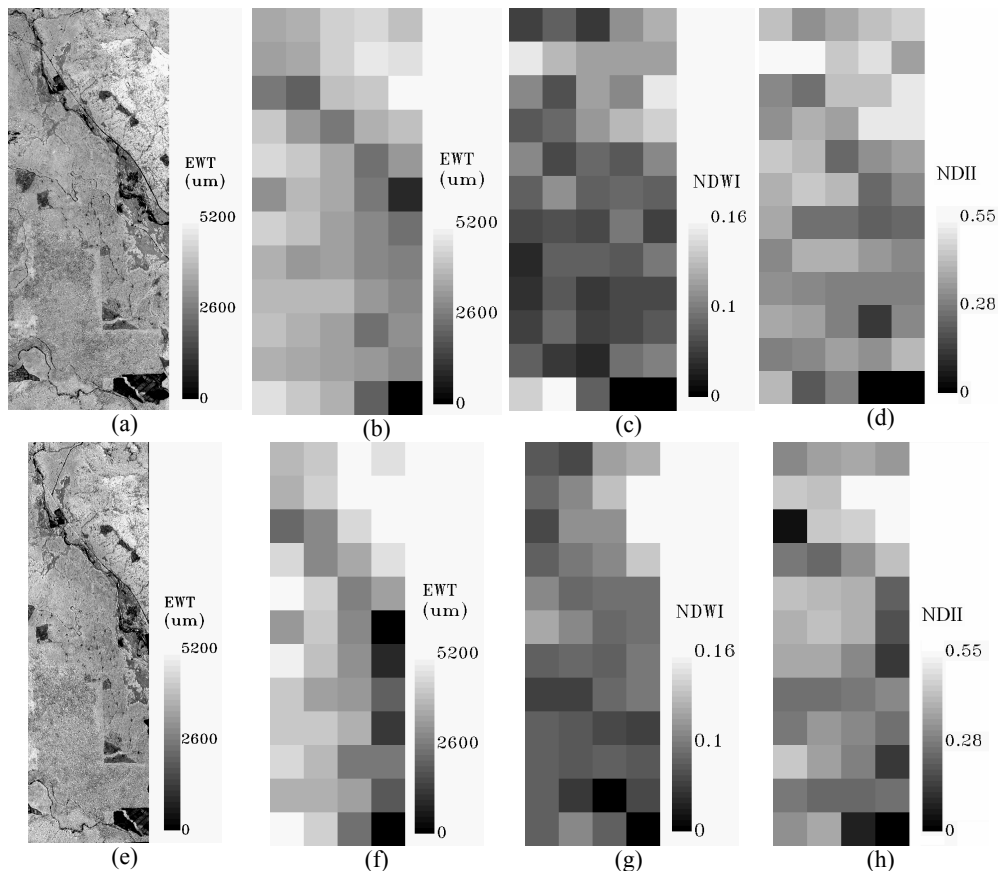


Fig. 4. (a) EWT map developed from AVIRIS imagery on 19 July 2003 at its original 4m pixel resolution, (b) EWT map developed from AVIRIS imagery on 19 July 2003 and scaled to MODIS pixels, (c) NDWI map at Wind River developed from MODIS reflectance bands on 19 July 2003, (d) NDII map at Wind River developed from MODIS reflectance bands on 19 July 2003, (e) EWT map developed from AVIRIS imagery on 1 August 2002 at its original 4m pixel resolution, (f) EWT map developed from AVIRIS imagery on 1 August 2002 and scaled to MODIS pixels, (g) NDWI map at Wind River developed from MODIS reflectance bands on 1 August 2002, (h) NDII map at Wind River developed from MODIS reflectance bands on 1 August 2002.

and MODIS data although the scaling of the reflectance data may not be equivalent (the gray scale ranges do not precisely match). Nonetheless, large spatial variance in EWT is apparent.

3.4 Comparison between AVIRIS and MODIS Indexes

Water indexes calculated from AVIRIS and MODIS data were compared in order to assess data agreement, using AVIRIS as the reference. After cross-calibration of MODIS to AVIRIS to align the radiometric measurements (accounting for view geometry differences due to swath position and the eight day compositing), and simulating the MODIS band-passes and spatial resolution in AVIRIS data, the water indexes were compared. Fig. 5 shows the NDWI retrieved by MODIS and AVIRIS for each forest type for 2002 and 2003, showing that the regression line between MODIS NDWI and AVIRIS NDWI is close to the dashed one-to-one line. Based on this agreement between the instruments, comparisons were conducted on AVIRIS and MODIS images for 2002 and 2003 using NDII and NDVI indexes, which showed results consistent with Fig. 5 (NDII had $r^2=0.45$ to 0.85 with slopes= 0.91 to 1.18 , and NDVI had $r^2=0.50$ to 0.80 with slopes= 0.92 to 1.08). These results demonstrate that the data are spectrally comparable from MODIS and AVIRIS instruments. This result enabled a further assessment of the retrieval of water content from MODIS compared to AVIRIS EWT.

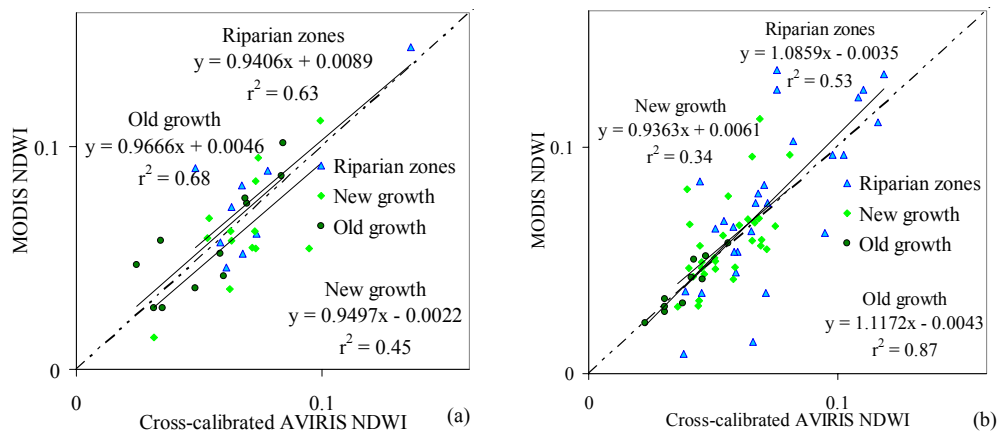


Fig. 5. (a) Comparison of NDWI retrieved from MODIS data and cross-calibrated AVIRIS data on 1 August 2002. (b) Comparison of NDWI retrieved from MODIS data and cross-calibrated AVIRIS data on 19 July 2003.

3.5 Comparison between NDVI, NDWI, NDII

Fig. 6 shows that MODIS NDVI, NDWI and NDII are linearly correlated to AVIRIS EWT, although with different slopes. This correlation allows MODIS canopy water content variation to be tracked and quantified over the growing season. The relationships for model-estimated AVIRIS EWT and MODIS NDVI, NDWI, and NDII for the three forests types are shown in Fig. 6. The coefficient of determination between the MODIS indexes and AVIRIS EWT varied from $r^2=0.25$ to 0.78 . Consistently, NDVI had the lowest regression correlation with EWT ($r^2=0.25$ to 0.35), NDWI produced a better correlation ($r^2=0.40$ to 0.44) and NDII had the best agreement with EWT for all three vegetation types ($r^2=0.50$ to 0.78).

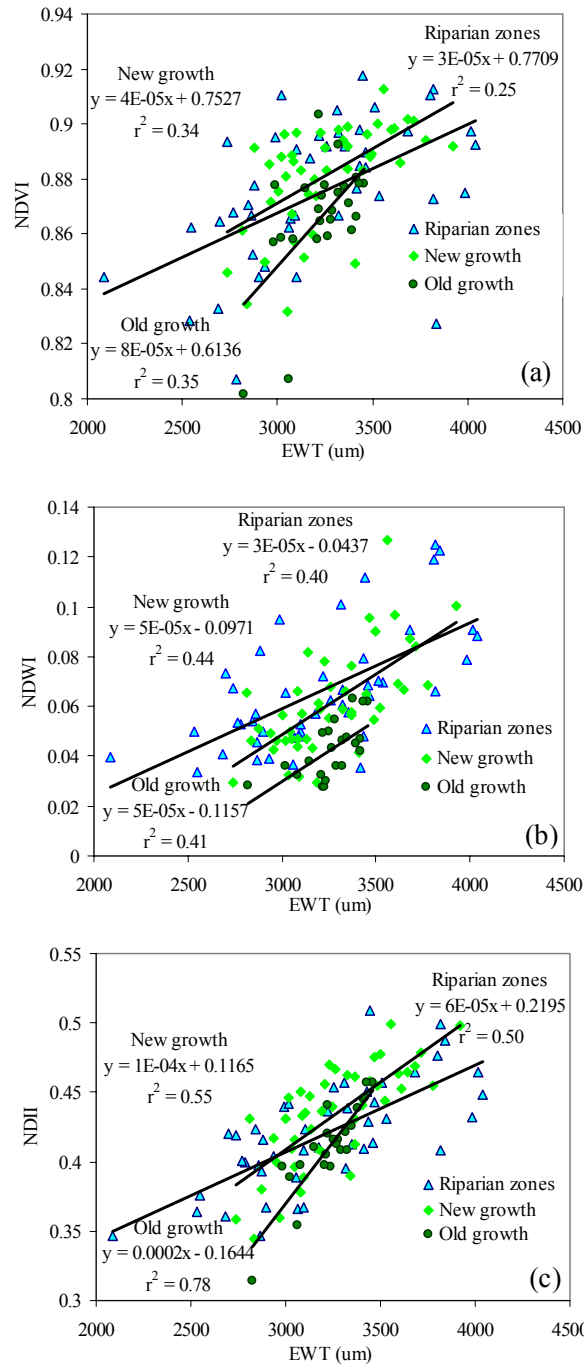


Fig. 6. Regression based on all years between (a) NDVI (b) NDWI and (c) NDII derived from MODIS reflectance and EWT derived from AVIRIS data for three major vegetation types at Wind River.

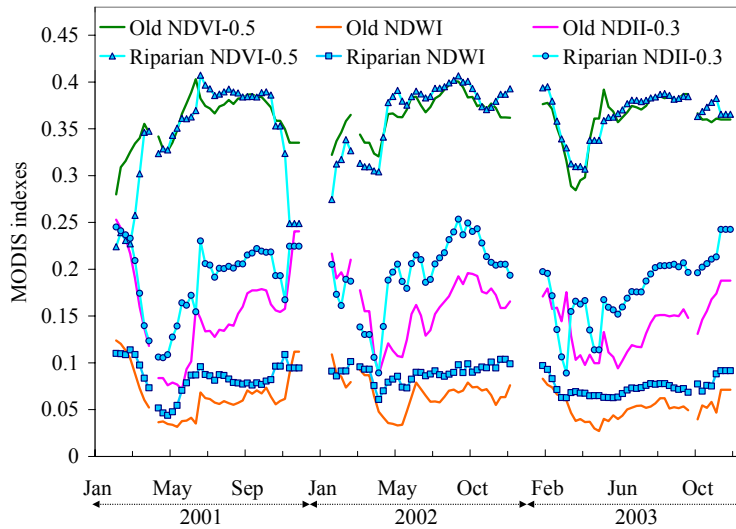


Fig. 7. Time series of NDVI, NDWI, and NDII derived from MODIS data in old growth conifer forests and riparian zones for three years (2001 through 2003). To fit the index scale, NDVI values are shown minus 0.5 and NDII values minus 0.3 of their true value.

The seasonal variation of NDVI, NDWI, and NDII was studied by deriving a time series of each index for each vegetation type from the three-year MODIS dataset (Fig. 7). NDVI, NDWI, and NDII were first calculated with MODIS reflectance data. The seasonal variations in the water indexes are similar to each other and comparable in timing and magnitude to the seasonal variation in precipitation. The seasonal variation of NDWI and NDII followed a distinctly different temporal trajectory than NDVI (Fig. 7). The water indexes were highest in winter and declined in spring, and increase again in the summer. Instead, NDVI was lowest in winter and spring (due to lower leaf area from needle loss and limited light interception), and only increases in late spring, following the annual leaf flush (late May-early June), and is highest in summer when leaf maturation is completed.

Previous studies have shown that MODIS water indexes provide information on canopy water content status [42]. As described in previous sections, photosynthetic activities of this old-growth conifer forest are strongly affected by seasonal changes in precipitation and water availability [63]. The correlation for the exchanges of water and carbon between plants and the atmosphere was also described. Based on these relationships, a comparison was made between the CO₂ flux measured at the AmeriFlux tower within the old growth conifer forest and the remotely sensed indexes, NDVI, NDWI, and NDII for the old growth conifer forest. NDVI begins its annual increase after the forest has become a carbon sink, although during the spring carbon sink period (Fig. 8a), and peaks significantly after the forest has become a source of carbon emissions. NDVI has low values when the sink strength is greatest. Therefore, the seasonal timing in NDVI does not correspond closely to the CO₂ flux. In contrast, these results show that the temporal trajectory in the water indexes do match the CO₂ flux trajectory during the period when the forest is a carbon sink, from late January to late May (Fig. 8b, c). Water indexes reach their minimum values concurrent with the peak uptake in net ecosystem exchange (NEE). The timing of the reverse trend, which increases water index values, occurs as NEE switches to becoming a CO₂ source. We hypothesize that this relationship is due to increasing cumulative water stress in the conifer canopies as a result of

stomatal opening for photosynthetic CO₂ uptake and concurrent loss of water from evapotranspiration during an environmental period of higher net radiation, higher temperatures, and lower precipitation.

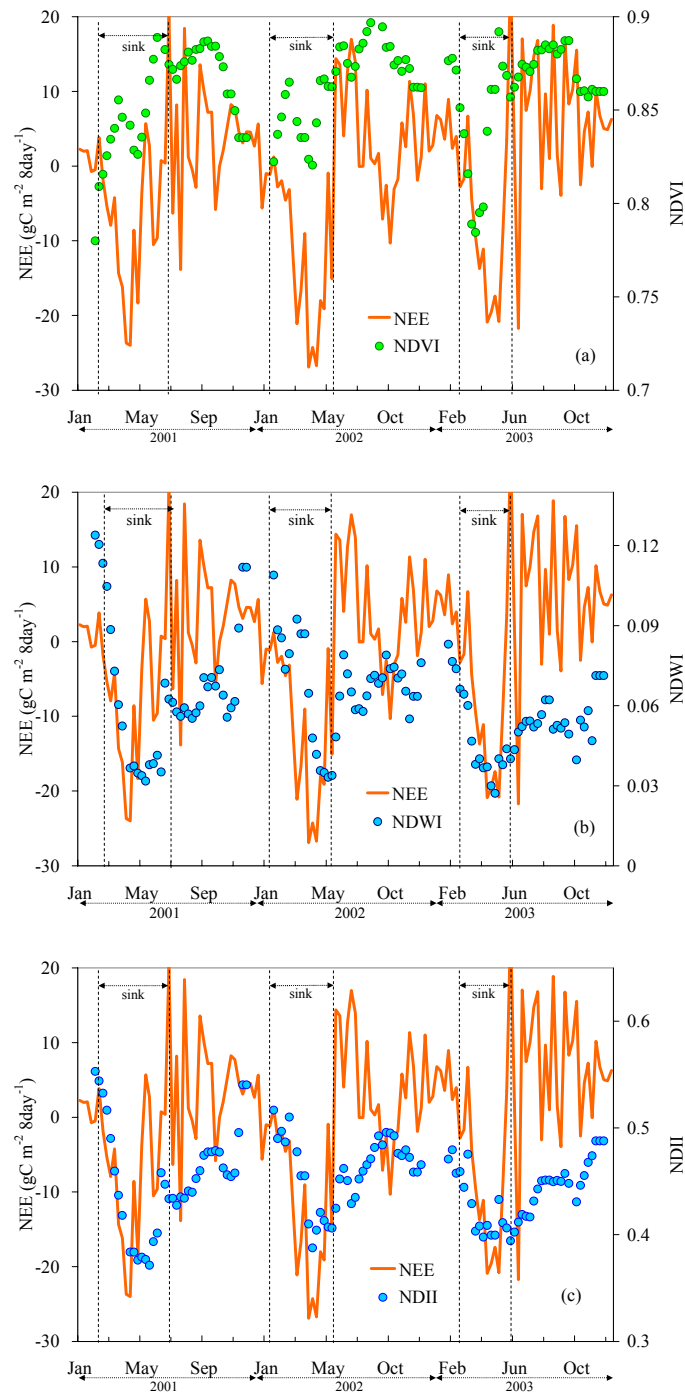


Fig. 8. Time series of MODIS (a) NDVI, (b) NDWI, and (c) NDII and NEE measured at Wind River Canopy Crane site.

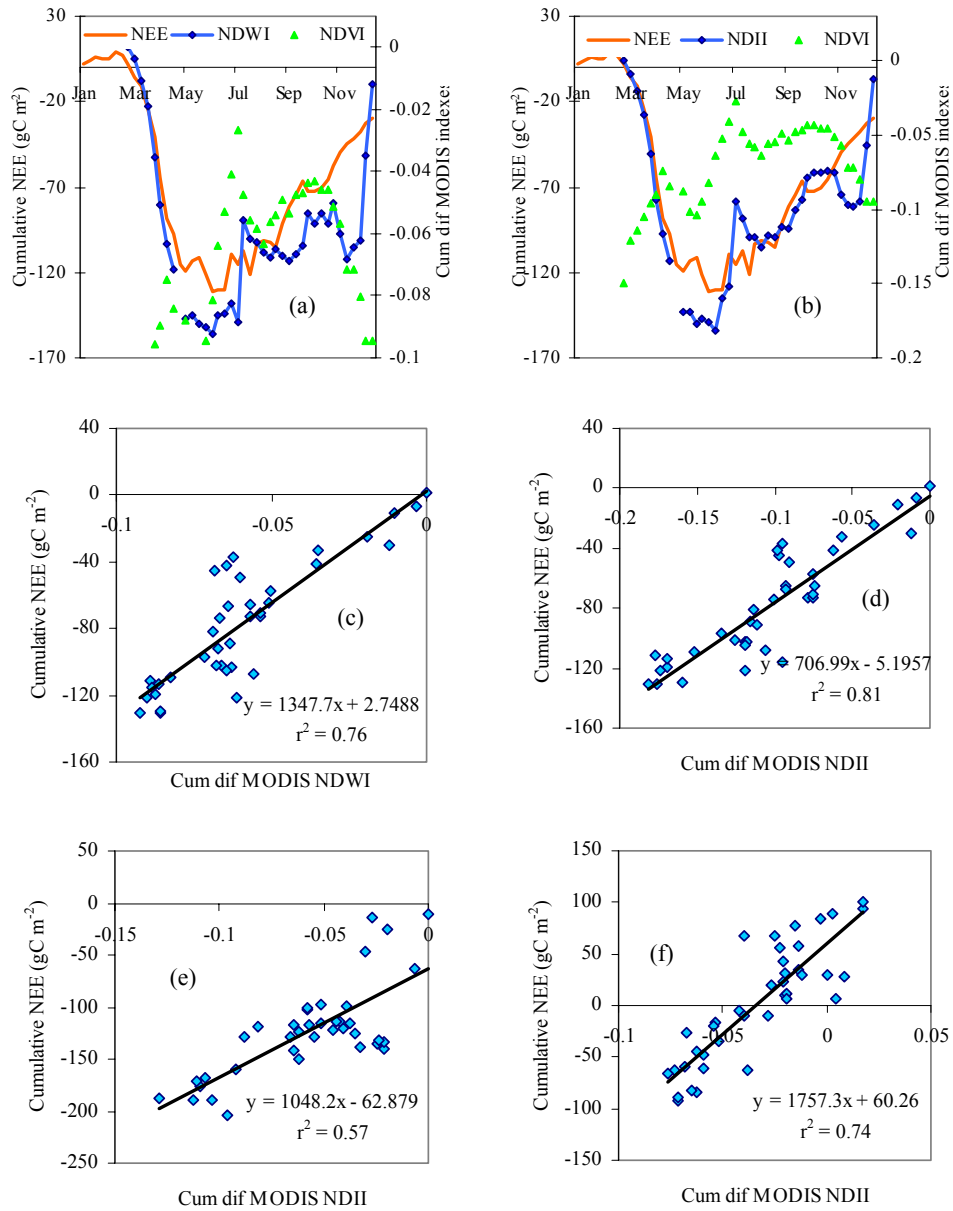


Fig. 9. (a),(b) Seasonal variation of cumulative NEE and cumulative difference MODIS NDVI, NDWI and NDII are shown for 2001. To fit the index scale, cumulative difference NDVI values are shown minus 0.15. (c) Regression for NDWI and NEE for 2001. Regressions for NDII and NEE for (d) 2001, (e) 2002, and (f) 2003.

To further explore the relationships between fluxes and the time series of NDVI, NDWI, and NDII, the cumulative fluxes were compared to the cumulative indexes for each year. We found similar seasonal variation between cumulative NEE and cumulative difference water indexes, using a 24-day time lag each year. The results for 2001 are shown in Fig. 9a,b. The

corresponding regressions for NDWI and NDII with NEE are shown in Fig. 9c,d. Both cumulative difference NDWI and NDII had similar linear regressions to cumulative NEE for the three years (Table 1). The temporal change in cumulative NEE and cumulative difference NDVI are shown in Fig. 9a,b. The regression correlations for cumulative difference NDVI with a 24-day time lag with cumulative NEE were not as good as regressions for NDWI and NDII for the three years (Table 1). However, this regression was improved by plotting cumulative difference NDVI with cumulative NEE with no time lag ($r^2=0.45, 0.39, 0.21$, respectively) although still remaining poorer than the water indexes.

The same analysis was applied to cumulative GPP, cumulative LE flux, cumulative H flux, and the three indexes. The regressions with GPP, LE, and H were non-linear with all three indexes, being of an order 2 polynomial. NDWI yielded a similar regression with cumulative GPP, a slightly poorer regression with LE and H (Table 1) for the three years. NDII had a similar regression correlation with cumulative GPP, LE, and a slightly poorer regression with H (Table 1). NDVI, however, had a better regression with GPP, LE and H than with NEE for the three years (Table 1). This counter intuitive result for the water indexes and LE appears to be a function of the phase differences between precipitation and temperature patterns and the temporal lag in the water indexes.

Table 1. Coefficient of determination for regressions between cumulative fluxes and cumulative difference MODIS indexes for 2001 through 2003. (Bold fonts indicate $p<0.005$ for the regression)

	NDVI			NDWI			NDII		
Year	2001	2002	2003	2001	2002	2003	2001	2002	2003
NEE	0.24	0.12	0.04	0.76	0.55	0.40	0.81	0.57	0.74
GPP	0.65	0.55	0.25	0.71	0.47	0.47	0.73	0.62	0.74
LE	0.66	0.60	0.32	0.67	0.37	0.47	0.70	0.47	0.72
H	0.60	0.60	0.39	0.51	0.48	0.22	0.54	0.68	0.48

The significant regressions between MODIS NDII and NEE were utilized to demonstrate potential applications of this empirical model. We applied the relationship between MODIS NDII and NEE developed in Fig. 9d,e,f to generate a cumulative spatially resolved NEE map at Wind River for the months of June and November in 2001, 2002, and 2003 (Fig. 10). In these figures, darker values indicate a more negative value of cumulative NEE (i.e., a greater carbon sink). Consistently, this simple model based on relationship to water indexes shows that the forest is a larger carbon sink in June (more dark pixels) than in November (more bright pixels) despite weather differences between years. Interannual differences are apparent in June 2002 which is darker in both June and November than either year 2001 or 2003, which is consistent with the higher NEE in 2002 (Table 2). Interestingly, in these three years, it is the old-growth forest in the bottom half of the image (see Fig. 3) that is the largest sink in both June and November and it is the riparian zone (upper right) that is the smallest sink for carbon. Cumulative NEE and from MODIS NDII in the old-growth conifer forest are shown in Table 2, which shows that the cumulative NEE values derived from the MODIS NDII are reasonable and comparable to measured NEE, with least differences in June relative to November. Among the three June maps (Fig. 10a,b,c), a somewhat smaller carbon sink is found for June 2001 in the old-growth forest which is also consistent with measured NEE (Fig. 1 and Table 2) and is mainly attributable to the far below normal precipitation during the 2000-2001 water year (Fig. 2). The flux measurements indicate that the old-growth forest was a weak-to-moderate carbon sink in year 2001 ($-30 \text{ gC m}^{-2} \text{ yr}^{-1}$) and 2002 ($-98 \text{ gC m}^{-2} \text{ yr}^{-1}$) and a moderate carbon source in 2003 ($+100 \text{ gC m}^{-2} \text{ yr}^{-1}$)[64]. The MODIS NDII-based cumulative NEE maps for November (Fig. 10 d,e,f) show higher NEE for November 2001 and 2002 (more dark pixels) than the map for November 2003 (more bright pixels). The MODIS-NDII-estimated cumulative NEE might enable us to investigate both the temporal and spatial variation of cumulative NEE for areas farther removed from the footprint of the

flux tower (i.e., to scale flux data to regional studies). However, one should consider that the relation between MODIS indexes and NEE were developed only for this specific old growth forest. Given the known differences in flux patterns between young and old growth Douglas-fir-western hemlock forests [78, 79], we expect different relationships must be developed between MODIS indexes and NEE for other land cover types. At this stage in development the relationships remain empirically calibrated.

Table 2. Comparisons between cumulative NEE derived from the Wind River AmeriFlux site and the MODIS NDII for June and November in 2001, 2002, and 2003.

	Cumulative NEE derived from flux tower data (gC m^{-2})	Cumulative NEE derived from MODIS NDII (gC m^{-2})
June 2001	-135	-134
Nov. 2001	-47	-64
June 2002	-170	-177
Nov. 2002	-114	-102
June 2003	-65	-53
Nov. 2003	73	54

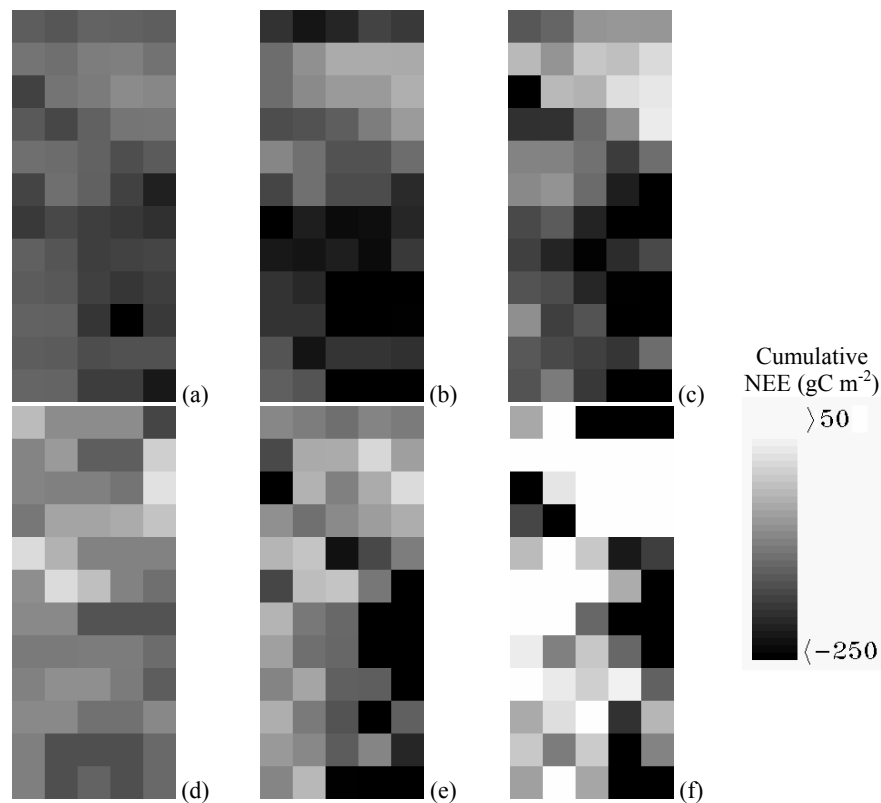


Fig. 10. MODIS-NDII-estimated cumulative NEE map for Wind River site in June (a) 2001, (b) 2002, (c) 2003, and November (d) 2001, (e) 2002, (f) 2003. The scale bar indicates the range of NEE.

4 DISCUSSION

We calculated and compared three MODIS indexes and AVIRIS EWT. In general, the old growth forest has a lower mean and range in each of the four indexes (EWT, NDVI, NDWI,

and NDII) while the riparian zones generally had the highest mean and largest range. These differences are largely attributed to the low albedo of the conifer forest (7.5%) [80] and the higher albedo of the broadleaf vegetation [29]. This pattern is seen in the spectra shown in Fig. 3b, and comparison of the forest classes (Fig. 3c) with the pixel spectra in Fig. 3a which are darker (lower values) in the old growth forest and brighter (higher values) in the riparian zones. In addition, for a given EWT, the three MODIS indexes (NDVI, NDWI, and NDII) are lower in the old growth than the other classes (Fig. 6).

Moreover, the slopes between the two water indexes and EWT are generally steeper for NDII (Fig. 6b, c), indicating that NDWI and NDII are more sensitive to changes in EWT than NDVI. NDVI has been reported to be sensitive to canopy gaps and shadows [29] and this perhaps accounts for the steeper NDVI slope in old growth forests than in other age class forests (Fig. 6a). NDVI is not directly sensitive to water which only absorbs at wavelengths longer than 1000 nm. The relationship between NDVI and water content assumes a constant relationship to chlorophyll concentration and in environments where NDVI tracks water content, it is because of the co-location of water and pigments in plant leaves and because the pigment index responds to variation in leaf area.

Two reasons could explain why NDII had a better correlation coefficient to EWT than NDWI in all three major forest types. The spectral region from 1550 to 1750 nm is best suited for leaf water content retrieval [45, 81-83]. Consistent with this, MODIS band 6 (1640 nm) was demonstrated by radiative transfer modeling to be more sensitive to variation of leaf water content [39] but is also sensitive to soil moisture [19, 56, 84] while MODIS band 5 was minimally affected by soil moisture. As a result, NDII had a larger dynamic range than NDWI. However, even in dense forest stands like these it is unlikely to have a completely closed canopy over a 500m-by-500m pixel. This is especially true in the regrowing forests that are widespread over this region [29], thus it is likely that variation in soil moisture affects the NDII measurement. The band 5 water absorption feature is enhanced by the high NIR scattering in the leaf, hence, the NDWI is sensitive to changes in liquid water content of vegetation canopies, and relatively insensitive to soil surface moisture [84].

We calculated a time series for the three MODIS indexes for each vegetation type. In summer, the riparian class had higher values in all three indexes than the old growth conifer forest (Fig. 7). However, in winter, the riparian vegetation had lower NDVI and NDWI than the old growth conifer forests, which likely resulted from leaf senescence and winter dormancy in this zone, which is dominated by deciduous woody species such as bigleaf maple (*Acer macrophyllum*), vine maple (*Acer circinatum*), and red alder (*Alnus rubra*). In contrast, the evergreen conifers retain leaves throughout the year, limiting winter decline in NDVI. However, during the winter of 2002 - 2003, NDVI and NDWI were both higher in the deciduous riparian zone than in the old growth conifer forest. The meteorological data show that this was an unusually warm winter (Fig. 2). Shaw *et al.* [57] report average January monthly air temperatures of 0.1°C while the monthly air temperature during this period was 6.6°C. Therefore, leaf senescence may have been less complete than typical or winter grasses could have grown and developed canopies, compared to less vegetation activity in cooler years.

NDVI (Fig. 8a) is at its lowest from February to April and generally increases over the period from March to October, before declining again. By early October, water indexes start to increase with the onset of autumn precipitation, and they reach their highest values in winter, concurrent with the peak in annual precipitation and when evaporative demands are low. Both water indexes decreased progressively from the time MODIS measurements could be resumed in February (when sufficient days without warning flags occurred) and reached lows in March. NDWI and NDII remained at low values for the period from March to May (Fig. 8b,c) and then increased to intermediate values where they remained during the summer drought when the canopy is under higher water stress conditions. Winner *et al.* [85] measured needle water potential in the upper canopy of old growth Douglas-fir at this site in

1999. They report that midday leaf water potentials also reach seasonal lowest (stressed) values by March and then remain consistently low throughout the summer into September [85], a temporal pattern similar to the water indexes during late spring and summer months.

As described above, the temporal trajectory in the water indexes match the CO₂ flux trajectory for the period when the forest is a carbon sink, from late January to late May. The reversal of the decline in the water indexes occurs in late May, and then gradually increase throughout the summer, reaching a maximum after autumn rains begin (Fig. 8b,c). This pattern of increasing water content during summer was unexpected since soil water content remains low or declines throughout this period. However, for this part of the seasonal cycle, the increase in water indexes co-occurs with the increase in NDVI ($r^2=0.55-0.66$, $p<0.0003$ for NDWI; $r^2=0.66-0.91$, $p<0.0001$ for NDII). The timing of this part of the seasonal pattern is consistent with an increase in leaf area. Douglas fir and other conifers break needle buds in late May (an average of 23 May (17-27 May) based on phenology data at this site, collected from 1997 through 2004, Ken Bible, unpublished data) and the observed increase in canopy water content may be due to hydration and maturation of the new needles. Leaf maturation at Wind River generally coincides with terminal bud formation, typically occurring during the last two week of June (K. Bible, unpublished data).

Biometeorological data collected at the crane in 1999, 2000, and 2004 show that soil moisture reaches maximum values in winter and starts to decline in spring. Soil moisture declines dramatically by late May or early June when winter precipitation ends. Soil moisture then continuously decreases through September, when it reaches a minimum. After the onset of fall precipitation, soil moisture begins to increase again by October. As a result of decreasing soil moisture in late spring, the forest moves from a net carbon sink to a source by summer and becomes a net carbon sink again early in the following calendar year (Fig. 8).

5 CONCLUSIONS

We demonstrate, for the first time, that water indexes can be used to monitor ecosystem fluxes in a high biomass western conifer forest in the Pacific Northwest. In this study, we demonstrated two forms of water indexes can be retrieved from coarse-scale MODIS data that are comparable to equivalent water thickness derived from fine spatial resolution hyperspectral AVIRIS data. The indexes exhibited different slopes depending on vegetation type and year, although their relative relationships remained consistent. The NDII index performed better than NDWI for estimating canopy water content. Canopy water content decreased during the spring reaching a minimum in May. Subsequent increases in NDII and NDWI coincided with the seasonal increase in NDVI, following the same trajectory as NDVI over the summer months ($r^2=0.55-0.91$). This water content pattern is not consistent with soil moisture, which remains low during summer months, but appears to be indicative of the higher leaf area in summer. NDVI was a poor indicator of canopy water content as expected for an index using visible and near-infrared bands without direct sensitivity to water. NDVI appears to follow the phenological cycle and the timing of bud break rather than the NEE cycle. It increases following bud break, reaching an annual maximum by autumn, then decreases until the next spring.

We explored the correlation in temporal variation between flux data and the three indexes, NDWI, NDII and NDVI and found markedly similar temporal patterns between NEE and water indexes, especially during periods when the forests were a net carbon sink. Further analysis on flux data and the MODIS water indexes showed that water indexes are highly correlated with similar regressions to net ecosystem exchange (NEE) and water exchange (LE). However, surprisingly NDVI had a poor correlation with CO₂ flux although a weak but better correlation with LE. These results demonstrate that the water and vegetation indexes derived from MODIS data can be used to track NEE and LE fluxes which will allow spatial

extension of data from flux towers to be scaled to regional estimates, at least for temperate and boreal conifer forests.

Acknowledgments

The authors gratefully acknowledge Dar Roberts (University of California, Santa Barbara) for providing forest age information and AVIRIS data used in this study and Ken Bible (University of Washington) for providing climate, forest phenology, and geographical information at the Wind River forest used in this study. Portions of this study were supported by National Aeronautics and Space Administration (NASA) under grant # NNG04GQ42G "Global Estimation of Canopy Water Content" and Contract # NAG5-9360 "New EOS Data Products to Improve Biogeochemical Estimates" and by the Office of Science (BER), U.S. Department of Energy, through the Western Regional Center of the National Institute for Global Environmental Change under Cooperative Agreements No. DE-FC03-90ER61010 and DE-FC02-03ER63613. The anonymous reviewers are gratefully acknowledged for their thoughtful critiques and suggestions.

References

- [1] P. J. Sellers, "Canopy reflectance, photosynthesis and transpiration," *Int. J. Rem. Sens.* **6**, 1335-1372 (1985).
- [2] S. L. Ustin, C. A. Wessman, B. Curtiss, E. Kasischke, J. Way, and V. C. Vanderbilt, "Opportunities for using the EOS imaging spectrometers and synthetic aperture radar in ecological models," *Ecology* **72**, 1934-1945 (1991).
- [3] J. Peñuelas, I. Filella, C. Biel, L. Serrano and R. Savé, "The reflectance at the 950-970 nm region as an indicator of plant water status," *Int. J. Rem. Sens.* **14**, 1887-1905 (1993).
- [4] S. L. Ustin, M. O. Smith, and J. B. Adams, "Remote sensing of ecological processes, a strategy for developing and testing ecological models using spectral mixture analysis," in *Scaling Physiological Processes, Leaf to Globe*, J. R. Ehleringer and C. B. Field, Eds., pp. 339-357, Academic Press, Inc., San Diego, CA (1993).
- [5] J. W. Rouse, R. H. Hass, J. A. Schell, and D. W. Deering, "Monitoring vegetation systems in the Great Plains with ERTS," in *Proc., Third Earth Resources Technology Satellite-1 Symp.*, Goddard Space Flight Centre, NASA., SP-351. 3010-3317 (1973).
- [6] P. J. Sellers, D. A. Randall, G. J. Collatz, J. A. Berry, C. B. Field, D. A. Dazlich, C. Zhang, G. D. Collelo, and L. Bounoua, "A revised land surface parameterization (SiB2) for atmospheric GCMS. Part II: the generation of global fields of terrestrial biophysical parameters from satellite data," *J. Clim.* **9**, 706-737 (1996) [doi: 10.1175/1520-0442(1996)009<0706:ARLSPF>2.0.CO;2].
- [7] B. K. Wylie, D. J. Meyer, L. L. Tieszen, and S. Mannel, "Satellite mapping of surface biophysical parameters at the biome scale over the North American grasslands, a case study," *Rem. Sens. Environ.* **79**, 266-278 (2002) [doi:10.1016/S0034-4257(01)00278-4].
- [8] G. Asrar, M. Fuchs, E. T. Kanemasu, and J. L. Hatfield, "Estimating absorbed photosynthetic radiation and leaf area index from spectral reflectance in wheat," *Agron. J.* **76**, 300-306 (1984).
- [9] C. J. Tucker, "Red and photographic infrared linear combinations for monitoring vegetation," *Rem. Sens. Environ.* **8**, 127-150 (1979) [doi:10.1016/0034-4257(79)90013-0].
- [10] C. J. Tucker, "Satellite remote sensing of total herbaceous biomass production in the Senegal Sahel, 1980-1984," *Rem. Sens. Environ.* **17**, 233-249 (1985) [doi:10.1016/0034-4257(85)90097-5].

- [11] J. A. Gamon, C. B. Field, M. L. Goulden, K. L. Griffin, A. E. Hartley, G. Joel, J. Peñuelas, and R. Valentini, "Relationships between NDVI, canopy structure, and photosynthesis in three Californian vegetation types," *Ecol. Appl.* **5**, 28-41 (1995) [doi:10.2307/1942049].
- [12] B.-C. Gao, "NDWI--A normalized difference water index for remote sensing of vegetation liquid water from space," *Rem. Sens. Environ.* **58**, 257-266 (1996) [doi:10.1016/S0034-4257(96)00067-3].
- [13] J. A. Gamon, C. B. Field, D. A. Roberts, S. L. Ustin, and R. Valentini, "Functional patterns in an annual grassland during an AVIRIS overflight," *Rem. Sens. Environ.* **44**, 239-253 (1993) [doi:10.1016/0034-4257(93)90019-T].
- [14] J. Peñuelas, J. A. Gamon, K. L. Griffin, and C. B. Field, "Assessing community type, plant biomass, pigment composition, and photosynthetic efficiency of aquatic vegetation from spectral reflectance," *Rem. Sens. Environ.* **46**, 110-118 (1993) [doi:10.1016/0034-4257(93)90088-F].
- [15] J. Peñuelas, J. A. Gamon, A. L. Fredeen, J. Merino, and C. B. Field, "Reflectance indices associated with physiological changes in nitrogen- and water-limited sunflower leaves," *Rem. Sens. Environ.* **48**, 135-146 (1994) [doi:10.1016/0034-4257(94)90136-8].
- [16] P. J. Sellers, "Canopy reflectance, photosynthesis, and transpiration, II. The role of biophysics in the linearity of their interdependence," *Rem. Sens. Environ.* **21**, 143-183 (1987) [doi:10.1016/0034-4257(87)90051-4].
- [17] C. J. Tucker, J. R. G. Townshend and T. E. Golf, "African landcover classification using satellite data," *Science* **227**, 369-375 (1985) [doi:10.1126/science.227.4685.369].
- [18] P. J. Sellers, C. J. Tucker, G. J. Collatz, S. O. Los, C. O. Justice, D. A. Dazlich, and D. A. Randall, "A global 1° by 1° NDVI data set for climate studies, 2. The generation of global fields of terrestrial biophysical parameters from the NDVI," *Int. J. Rem. Sens.* **15**, 3519-3545 (1994).
- [19] X. Xiao, S. Boles, J. Liu, D. Zhuang, S. Froking, C. Li, W. Salas, and B. Moore III, "Mapping paddy rice agriculture in southern China using multi-temporal MODIS images," *Rem. Sens. Environ.* **95**, 480-492 (2005) [doi:10.1016/j.rse.2004.12.009].
- [20] P. J. Sellers, Y. Mintz, Y. C. Sud, and A. Dalcher, "A Simple Biosphere Model (SiB) for Use within General Circulation Models," *J. Atmos. Sci.* **43**, 505-531 (1986) [doi:10.1175/1520-0469(1986)043<0505:ASBMFU>2.0.CO;2].
- [21] P. J. Sellers, D. A. Randall, G. J. Collatz, J. A. Berry, C. B. Field, D. A. Dazlich, C. Zhang, G. D. Collelo, and L. Bounoua, "A revised land surface parameterization (SiB2) for atmospheric GCMS. Part I: model formulation," *J. Clim.* **9**, 676-705 (1996) [doi: 10.1175/1520-0442(1996)009<0676:ARLSPF>2.0.CO;2].
- [22] D. Stow, A. Hope, W. Boynton, S. Phinn, D. Walker, and N. Auerbach, "Satellite-derived vegetation index and cover type maps for estimating carbon dioxide flux for arctic tundra regions," *Geomorphology* **21**, 313-327 (1998) [doi:10.1016/S0169-555X(97)00071-8].
- [23] E. Boegh, H. Soegaard, N. Hanan, P. Kabat, and L. Lesch, "A remote sensing study of the NDVI-Ts relationship and the transpiration from sparse vegetation in the Sahel based on high-resolution satellite data," *Rem. Sens. Environ.* **69**, 224-240 (1999) [doi:10.1016/S0034-4257(99)00025-5].
- [24] B. K. Wylie, D. A. Johnson, E. Laca, N. Z. Saliendra, T. G. Gilmanov, B. C. Reed, L. L. Tieszen, and B. B. Worstell, "Calibration of remotely sensed, coarse resolution NDVI to CO₂ fluxes in a sagebrush-steppe ecosystem," *Rem. Sens. Environ.* **85**, 243-255 (2003) [doi:10.1016/S0034-4257(03)00004-X].
- [25] I. Filella, J. Peñuelas, L. Llorens, and M. Estiarte, "Reflectance assessment of seasonal and annual changes in biomass and CO₂ uptake of a Mediterranean

- shrubland submitted to experimental warming and drought," *Rem. Sens. Environ.* **90**, 308-318 (2004) [doi:10.1016/j.rse.2004.01.010].
- [26] S. W. Running and S. T. Gower, "FOREST-BGC, A general model of forest ecosystem processes for regional applications. II. Dynamic carbon allocation and nitrogen budgets," *Tree Physiol.* **9**, 147-160 (1991).
- [27] S. W. Running and R. R. Nemani, "Relating seasonal patterns of the AVHRR vegetation index to simulated photosynthesis and transpiration of forests in different climates," *Rem. Sens. Environ.* **24**, 347-367 (1988) [doi:10.1016/0034-4257(88)90034-X].
- [28] K. F. Huemmrich, T. A. Black, P. G. Jarvis, J. H. McCaughey, and F. G. Hall, "High temporal resolution NDVI phenology from micrometeorological radiation sensors " *J. Geophys. Res.* **104**, 27,935-927,944 (1999) [doi: 10.1029/1999JD900164].
- [29] D. A. Roberts, S. L. Ustin, S. Ogunjemiyo, J. Greenberg, S. Z. Dobrowski, J. Chen, and T. M. Hinckley, "Spectral and structural measures of northwest forest vegetation at leaf to landscape scales," *Ecosystems* **7**, 545-562 (2004) [doi:10.1007/s10021-004-0144-5].
- [30] O. Lillesaeter, "Spectral reflectance of partly transmitting leaves: Laboratory measurements and mathematical modeling," *Rem. Sens. Environ.* **12**, 247-254 (1982) [doi:10.1016/0034-4257(82)90057-8].
- [31] F. Baret and G. Guyot, "Potentials and limits of vegetation indices for LAI and APAR assessment," *Rem. Sens. Environ.* **35**, 161-173 (1991) [doi:10.1016/0034-4257(91)90009-U].
- [32] X. Gao, A. R. Huete, W. Ni, and T. Miura, "Optical-biophysical relationships of vegetation spectra without background contamination," *Rem. Sens. Environ.* **74**, 609-620 (2000) [doi:10.1016/S0034-4257(00)00150-4].
- [33] A. R. Huete, K. Didan, T. Miura, E. P. Rodriguez, X. Gao, and L. G. Ferreira, "Overview of the radiometric and biophysical performance of the MODIS vegetation indices," *Rem. Sens. Environ.* **83**, 195-213 (2002) [doi:10.1016/S0034-4257(02)00096-2].
- [34] A. R. Huete, R. D. Jackson, and D. F. Post, "Spectral response of a plant canopy with different soil backgrounds," *Rem. Sens. Environ.* **17**, 37-53 (1985) [doi:10.1016/0034-4257(85)90111-7].
- [35] A. R. Huete, H. Q. Liu, K. Batchily, and W. van Leeuwen, "A comparison of vegetation indices over a global set of TM images for EOS-MODIS," *Rem. Sens. Environ.* **59**, 440-451 (1997) [doi:10.1016/S0034-4257(96)00112-5].
- [36] X. Xiao, B. Braswell, Q. Zhang, S. Boles, S. Frolking, and B. Moore III, "Sensitivity of vegetation indices to atmospheric aerosols: continental-scale observations in Northern Asia," *Rem. Sens. Environ.* **84**, 385-392 (2003) [doi:10.1016/S0034-4257(02)00129-3].
- [37] B.-C. Gao and A. F. H. Goetz, "Retrieval of equivalent water thickness and information related to biochemical components of vegetation canopies from AVIRIS data," *Rem. Sens. Environ.* **52**, 155-162 (1995) [doi:10.1016/0034-4257(95)00039-4].
- [38] J. Peñuelas, J. Piñol, R. Ogaya, and I. Filella, "Estimation of plant water concentration by the reflectance Water Index WI (R900/R970)," *Int. J. Rem. Sens.* **18**, 2869-2875 (1997) [doi: 10.1080/014311697217396].
- [39] P. J. Zarco-Tejada, C. A. Rueda, and S. L. Ustin, "Water content estimation in vegetation with MODIS reflectance data and model inversion methods," *Rem. Sens. Environ.* **85**, 109-124 (2003) [doi:10.1016/S0034-4257(02)00197-9].
- [40] S. L. Ustin, D. A. Roberts, J. Pinzón, S. Jacquemoud, M. Gardner, G. Scheer, C. M. Castaneda, and A. Palacios-Orueta, "Estimating canopy water content of chaparral

- shrubs using optical methods," *Rem. Sens. Environ.* **65**, 280-291 (1998) [doi:10.1016/S0034-4257(98)00038-8].
- [41] S. L. Ustin, D. Darling, S. Kefauver, J. Greenberg, Y.-B. Cheng, and M. L. Whiting, "Remotely sensed estimates of crop water demand," in *Remote Sensing and Modeling of Ecosystems for Sustainability*, W. Gao and D. R. Shaw, Eds., Proc. SPIE **5544**, 230-240 (2004). [doi:10.1117/12.560309]
- [42] S. L. Ustin, S. Jacquemoud, P. J. Zarco-Tejada, and G. P. Asner, "Remote Sensing of Environmental Processes, State of the Science and New Directions," in *Manual of Remote Sensing Vol. 4., Remote Sensing for Natural Resource Management and Environmental Monitoring*, S. L. Ustin, Ed., 679-730, ASPRS. John Wiley and Sons, New York (2004).
- [43] P. J. Sellers, R. E. Dickinson, D. A. Randall, A. K. Betts, F. G. Hall, J. A. Berry, G. J. Collatz, A. S. Denning, H. A. Mooney, C. A. Nobre, N. Sato, C. B. Field, and A. Henderson-Sellers, "Modeling the exchange of energy, water, and carbon between continents and the atmosphere," *Science* **275**, 502-509 (1997) [doi:10.1126/science.275.5299.502].
- [44] I. Baker, A. S. Denning, N. Hanan, L. Prihodko, M. Uliasz, P.-L. Vidale, K. Davis, and P. Bakwin, "Simulated and observed fluxes of sensible and latent heat and CO₂ at the WLEF-TV tower using SiB2.5," *Global Change Biol.* **9**, 1262-1277 (2003) [doi:10.1046/j.1365-2486.2003.00671.x].
- [45] S. Jacquemoud, S. L. Ustin, J. Verdebout, G. Schmuck, G. Andreoli, and B. Hosgood, "Estimating leaf biochemistry using the PROSPECT leaf optical properties model," *Rem. Sens. Environ.* **56**, 194-202 (1996) [doi:10.1016/0034-4257(95)00238-3].
- [46] E. R. Hunt Jr. and B. N. Rock, "Detection of changes in leaf water content using Near- and Middle-Infrared reflectances," *Rem. Sens. Environ.* **30**, 43-54 (1989) [doi:10.1016/0034-4257(89)90046-1].
- [47] P. J. Zarco-Tejada and S. L. Ustin, "Modeling Canopy Water Content for Carbon Estimates from MODIS data at Land EOS Validation Sites," in *the IEEE 2001 International Geoscience and Remote Sensing Symposium, IGARSS'01, Sydney, Australia*. 9-13, July.
- [48] R. Fensholt and I. Sandholt, "Derivation of a shortwave infrared water stress index from MODIS near- and shortwave infrared data in a semiarid environment," *Rem. Sens. Environ.* **87**, 111-121 (2003) [doi:10.1016/j.rse.2003.07.002].
- [49] X. Xiao, Q. Zhang, B. Braswell, S. Urbanski, S. Boles, S. Wofsy, B. Moore III, and D. Ojima, "Modeling gross primary production of temperate deciduous broadleaf forest using satellite images and climate data," *Rem. Sens. Environ.* **91**, 256-270 (2004) [doi:10.1016/j.rse.2004.03.010].
- [50] S. Jacquemoud and F. Baret, "PROSPECT: a model of leaf optical properties spectra," *Rem. Sens. Environ.* **34**, 75-91 (1990) [doi:10.1016/0034-4257(90)90100-Z].
- [51] M. Zhang, S. L. Ustin, E. Rejmankova, and E. W. Sanderson, "Monitoring Pacific coast salt marshes using remote sensing," *Ecol. Appl.* **7**, 1039-1053 (1997).
- [52] E. W. Sanderson, M. Zhang, S. L. Ustin, and E. Rejmankova, "Geostatistical scaling of canopy water content in a California salt marsh," *Landscape Ecol.* **13**, 79-92 (1998) [doi:10.1023/A:1007961516096].
- [53] L. Serrano, S. L. Ustin, D. A. Roberts, J. A. Gamon, and J. Peñuelas, "Deriving water content of chaparral vegetation from AVIRIS data," *Rem. Sens. Environ.* **74**, 570-581 (2000) [doi:10.1016/S0034-4257(00)00147-4].
- [54] M. A. Hardisky, V. Klemas, and R. M. Smart, "The influence of soil salinity, growth form, and leaf moisture on the spectral reflectance of *Spartina alternifolia* canopies," *Photogram. Eng. Rem. Sensing* **49**, 77-83 (1983).

- [55] X. Xiao, S. Boles, J. Liu, D. Zhuang, and M. Liu, "Characterization of forest types in Northeastern China, using multi-temporal SPOT-4 VEGETATION sensor data," *Rem. Sens. Environ.* **82**, 335-348 (2002) [doi:10.1016/S0034-4257(02)00051-2].
- [56] X. Xiao, Q. Zhang, S. Saleska, L. Hutya, P. De Camargo, S. Wofsy, S. Frolking, S. Boles, M. Keller, and B. Moore III, "Satellite-based modeling of gross primary production in a seasonally moist tropical evergreen forest," *Rem. Sens. Environ.* **94**, 105-122 (2005) [doi:10.1016/j.rse.2004.08.015].
- [57] D. C. Shaw, J. F. Franklin, K. Bible, J. Klopatek, E. Freeman, S. Greene, and G. G. Parker, "Ecological setting of the Wind River old-growth forest," *Ecosystems* **7**, 427-439 (2004) [doi:10.1007/s10021-004-0135-6].
- [58] G. G. Parker, M. E. Harmon, M. A. Lefsky, J. Chen, R. V. Pelt, S. B. Weis, S. C. Thomas, W. E. Winner, D. C. Shaw, and J. F. Franklin, "Three-dimensional structure of an old-growth *Pseudotsuga-Tsuga* canopy and its implications for radiation balance, microclimate, and gas exchange," *Ecosystems* **7**, 440-453 (2004) [doi:10.1007/s10021-004-0136-5].
- [59] M. E. Harmon, K. Bible, M. G. Ryan, D. C. Shaw, H. Chen, J. Klopatek, and X. Li, "Production, respiration, and overall carbon balance in an old-growth *Pseudotsuga Tsuga* forest ecosystem," *Ecosystems* **7**, 498-512 (2004) [doi:10.1007/s10021-004-0140-9].
- [60] J. F. Franklin, T. A. Spies, R. V. Pelt, A. B. Carey, D. A. Thornburgh, D. R. Berg, D. B. Lindenmayer, M. E. Harmon, W. S. Keeton, and D. C. Shaw, "Disturbances and structural development of natural forest ecosystems with silvicultural implications, using Douglas-fir forests as an example," *For. Eco. Manag.* **155**, 399-423 (2002) [doi:10.1016/S0378-1127(01)00575-8].
- [61] W. Hargrove and F. Hoffman, "Potential of multivariate quantitative methods for delineation and visualization of ecoregions," *Environ. Manag.* **34**, S39-S60 (2004) [doi:10.1007/s00267-003-1084-0].
- [62] T. H. Suchanek, H. A. Mooney, J. F. Franklin, H. Gucinski, and S. L. Ustin, "Carbon dynamics of an old-growth forest," *Ecosystems* **7**, 421-426 (2004) [doi:10.1007/s10021-004-0134-7].
- [63] K. T. Paw U, M. Falk, T. H. Suchanek, S. L. Ustin, J. Chen, Y.-S. Park, W. E. Winner, S. C. Thomas, T. C. Hsiao, R. H. Shaw, T. S. King, R. D. Pyles, M. Schroeder, and A. A. Matista, "Carbon dioxide exchange between an old-growth forest and the atmosphere," *Ecosystems* **7**, 513-524 (2004) [doi:10.1007/s10021-004-0141-8].
- [64] M. Falk, Carbon and energy exchange between an old-growth forest and the atmosphere, Ph.D., Land, Air, and Water Resources, University of California, Davis (2005).
- [65] E. Falge, D. Baldocchi, R. Olson, P. Anthoni, M. Aubinet, C. Bernhofer, G. Burba, R. Ceulemans, R. Clement, and H. Dolman, "Gap filling strategies for defensible annual sums of net ecosystem exchange," *Ag. For. Meteorol.* **107**, 43-69 (2001) [doi:10.1016/S0168-1923(00)00225-2].
- [66] M. L. Goulden, J. W. Munger, S.-M. Fan, B. C. Daube, and S. C. Wofsy, "Measurements of carbon sequestration by long-term eddy covariance: methods and a critical evaluation of accuracy," *Global Change Biol.* **2**, 169-182 (1996) [doi:10.1111/j.1365-2486.1996.tb00070.x].
- [67] M. Reichstein, E. Falge, D. Baldocchi, D. Papale, M. Aubinet, P. Berbigier, C. Bernhofer, N. Buchmann, T. Gilmanov, A. Granier, T. Grunwald, K. Havrankova, H. Ilvesniemi, D. Janous, A. Knohl, T. Laurila, A. Lohila, D. Loustau, G. Matteucci, T. Meyers, F. Miglietta, J. Ourcival, J. Pumpanen, S. Rambal, E. Rotenberg, M. Sanz, J. Tenhunen, G. Seufert, F. Vaccari, T. Vesala, D. Yakir, and R. Valentini, "On the separation of net ecosystem exchange into assimilation and ecosystem

- respiration: review and improved algorithm," *Global Change Biol.* **11**, 1424-1439 (2005) [doi:10.1111/j.1365-2486.2005.001002.x].
- [68] R. O. Green, J. E. Conel, J. S. Margolis, C. J. Bruegge, and G. L. Hoover, "An inversion algorithm for retrieval of atmospheric and leaf water absorption from AVIRIS radiance with compensation for atmospheric scattering," in *Proceeding of the Third AVIRIS Workshop*; Eds., JPL Publication 91-28 p. (1991).
- [69] R. O. Green, J. E. Conel, and D. A. Roberts, "Estimation of aerosol optical depth & calculation of apparent surface reflectance from radiance measured by the airborne visible-infrared imaging spectrometer (AVIRIS) using MODTRAN2," in *Imaging Spectrometry of the Terrestrial Environment*, G. Vane, ed., Proc. SPIE **1937**, 2-11, (1993).
- [70] D. A. Roberts, R. O. Green, and J. B. Adams, "Temporal and spatial patterns in vegetation and atmospheric properties from AVIRIS," *Rem. Sens. Environ.* **62**, 223-240 (1997) [doi:10.1016/S0034-4257(97)00092-8].
- [71] D. A. Roberts, M. Gardner, R. Church, S. L. Ustin, G. Scheer, and R. O. Green, "Mapping Chaparral in the Santa Monica Mountains Using Multiple Endmember Spectral Mixture Models," *Rem. Sens. Environ.* **65**, 267-279 (1998) [doi:10.1016/S0034-4257(98)00037-6].
- [72] C. B. Field and J. Kaduk, "The carbon balance of an old-growth forest: Building across approaches," *Ecosystems* **7**, 525-533 (2004) [doi:10.1007/s10021-004-0142-7].
- [73] C. C. Barford, S. C. Wofsy, M. L. Goulden, J. W. Munger, E. H. Pyle, S. P. Urbanski, L. Hutya, S. R. Saleska, D. Fitzjarrald, and K. Moore, "Factors controlling long- and short- term sequestration of atmospheric CO₂ in a midlatitude forest," *Science* **294**, 1688-1691 (2001) [doi: 10.1126/science.1062962].
- [74] K. Morgenstern, T. Andrew Black, E. R. Humphreys, T. J. Griffis, G. B. Drewitt, T. Cai, Z. Nestic, D. L. Spittlehouse, and N. J. Livingston, "Sensitivity and uncertainty of the carbon balance of a Pacific Northwest Douglas-fir forest during an El Niño/La Niña cycle," *Ag. For. Meteorol.* **123**, 201-219 (2004) [doi:10.1016/j.agrformet.2004.03.008].
- [75] M. Falk, K. T. Paw U, S. Wharton, and M. Schroeder, "Is soil respiration a major contributor to the carbon budget within a Pacific Northwest old-growth forest?," *Ag. For. Meteorol.* **135**, 269-283 (2005) [doi:10.1016/j.agrformet.2005.12.005].
- [76] C. M. Champagne, K. Staenz, A. Bannari, H. McNairn, and J.-C. Deguise, "Validation of a hyperspectral curve-fitting model for the estimation of plant water content of agricultural canopies," *Rem. Sens. Environ.* **87**, 148-160 (2003) [doi:10.1016/S0034-4257(03)00137-8].
- [77] P. E. Dennison, D. A. Roberts, S. R. Thorgusen, J. C. Regelbrugge, D. Weise, and C. Lee, "Modeling seasonal changes in live fuel moisture and equivalent water thickness using a cumulative water balance index," *Rem. Sens. Environ.* **88**, 442-452 (2003) [doi:10.1016/j.rse.2003.08.015].
- [78] J. Chen, K. T. Paw U, S. L. Ustin, T. H. Suchanek, B. J. Bond, K. D. Brosofske, and M. Falk, "Net ecosystem exchanges of carbon, water, and energy in young and old-growth Douglas-fir forests," *Ecosystems* **7**, 534-544 (2004) [doi:10.1007/s10021-004-0143-6].
- [79] J. Chen, M. Falk, E. Euskirchen, K. T. Paw U, T. Suchanek, S. L. Ustin, B. Bond, N. Phillips, and K. Brosofske, "Biophysical controls of carbon flows in three successional Douglas-fir stands based upon eddy-covariance measurements," *Tree Physiol.* **22**, 169-177 (2001).
- [80] M. J. Mariscal, S. N. Martens, S. L. Ustin, J. Chen, S. B. Weiss, and D. A. Roberts, "Light-transmission profiles in an old-growth forest canopy: Simulations of

- photosynthetically active radiation by using spatially explicit radiative transfer models," *Ecosystems* **7**, 454-467 (2004) [doi:10.1007/s10021-004-0137-4].
- [81] C. J. Tucker, "Remote sensing of leaf water content in the near infrared," *Rem. Sens. Environ.* **10**, 23-32 (1980) [doi:10.1016/0034-4257(80)90096-6].
- [82] S. Jacquemoud and F. Baret, "Estimation des parametres biophysiques d'un couvert vegeta; par inversion d'un modele de reflectance sur des donnees haute resolution spectrale," in *Structure du couvert vegetal et climat lumineux. Methodes de caracterisation et applications*; Eds., p. (1991).
- [83] S. Jacquemoud, F. Baret, B. Andrieu, F. M. Danson, and K. Jaggard, "Extraction of Vegetation Biophysical Parameters by Inversion of the Prospect Plus Sail Models on Sugar Beet Canopy Reflectance Data - Application to TM and AVIRIS Sensors," *Rem. Sens. Environ.* **52**, 163-172 (1995) [doi:10.1016/0034-4257(95)00018-V].
- [84] A. R. Huete, "Estimation of Soil Properties Using Hyperspectral VIS/IR Sensors," in *Encyclopedia of Hydrological Sciences* M. G. Anderson, Ed., pp. 15, John Wiley & Sons, Ltd, New York (2005).
- [85] W. E. Winner, S. C. Thomas, J. A. Berry, B. J. Bond, C. E. Cooper, T. M. Hinckley, J. R. Ehleringer, J. E. Fessenden, B. Lamb, S. McCarthy, N. G. McDowell, N. Phillips, and M. Williams, "Canopy carbon gain and water use: analysis of old-growth conifers in the Pacific Northwest," *Ecosystems* **7**, 482-497 (2004) [doi:10.1007/s10021-004-0139-2].